

**THEORETICAL INVESTIGATION INTO THE REACTION MECHANISMS  
OF BENZYL ALCOHOL WITH DIMETHYL CARBONATE OVER A  
FAUJASITE ZEOLITE CATALYST**

**by**

**CHONG SHU XIAN**

**Thesis submitted in fulfillment of the requirements  
for the degree of  
Master of Science**

**March 2012**

## **ACKNOWLEDGEMENT**

During my research work I have been accompanied and supported by many people directly or indirectly. I am very pleased to express my gratitude to all of them.

First and foremost, I thank my main supervisor, Dr. Hassan Hadi Abdallah for his valuable advice, supervision, guidance, constant encouragement and support in every stage of this research. His editorial advice was vital to the completion of this work. He has always given me constructive suggestions and enlightened me in many ways to approach the research.

Special thanks to my co-supervisor, Prof. Dr. Habibah A. Wahab, from the School of Pharmaceutical Sciences, Universiti Sains Malaysia; for providing me precious opinions in my research work.

Endless thank to my beloved family for unconditional support and encouragement to pursue my interests. Finally, many thanks to my lab mates and everyone who have made things possible.

## TABLE OF CONTENTS

Acknowledgement.....	ii
Table of Contents.....	iii
List of Tables.....	vi
List of Figures.....	viii
List of Abbreviations.....	xii
List of Symbols.....	xiv
Abstrak.....	xv
Abstract.....	xvi

### CHAPTER I- INTRODUCTION

1.1 Introduction.....	1
1.2 Problem Statement.....	6
1.3 Significant of Research.....	6
1.4 Objectives.....	7
1.5 Scope of Research.....	7

### CHAPTER II- LITERATURE REVIEW

2.1 Introduction to Zeolite.....	8
2.2 Application of Zeolite.....	9
2.3 The Faujasite Zeolite Framework.....	12
2.4 Introduction to Computational Chemistry.....	15
2.4.1 Ab-initio Methods.....	16
2.4.2 Semiempirical Methods.....	18
2.4.3 Molecular Mechanics Methods.....	19
2.4.4 Quantum Mechanics/Molecular Mechanics Methods (QM/MM) Methods.....	20
2.5 Quantum Chemistry Software Packages.....	23
2.6 Theoretical Study By Applying A Hybrid QM/MM Method.....	24
2.7 Transition State Theory.....	27

### CHAPTER III- Methodology

3.1 Computer.....	29
-------------------	----

3.2	Procedures .....	29
-----	------------------	----

## CHAPTER IV- RESULTS AND DISCUSSION

4.1	Reaction Mechanisms between Benzyl Alcohol and DMC over a 3T (B3LYP/6-31g(d,p)) Quantum Cluster of Zeolite .....	32
4.1.1	Adsorption of Reactants onto The Zeolite Surface over a 3T (B3LYP/6-31g(d,p)) Quantum Cluster of Zeolite .....	32
4.1.2	Methylation of Benzyl Alcohol over a 3T (B3LYP/6-31g(d,p)) Quantum Cluster of Zeolite .....	37
4.1.2 (a)	Pathway 1: Methylation of Benzyl Alcohol with Two TS over a 3T (B3LYP/6-31g(d,p)) Quantum Cluster of Zeolite .....	37
4.1.2 (b)	Pathway 2: Methylation of Benzyl Alcohol with a Single TS over a 3T (B3LYP/6-31g(d,p)) Quantum Cluster of Zeolite .....	41
4.1.3	Carboxymethylation of Benzyl Alcohol over a 3T (B3LYP/6-31g(d,p)) Quantum Cluster of Zeolite .....	44
4.2	Reaction Mechanisms between Benzyl Alcohol and DMC over a 36T (ONIOM(HF/3-21g: UFF)) Quantum Cluster of Zeolite .....	49
4.2.1	Adsorption of Reactants onto the Zeolite Surface over a 36T (ONIOM(HF/3-21g: UFF)) Quantum Cluster of Zeolite .....	50
4.2.2	Methylation of Benzyl Alcohol over a 36T (ONIOM(HF/3-21g: UFF)) Quantum Cluster of Zeolite....	54
4.2.2 (a)	Pathway 1: Methylation of Benzyl Alcohol with Two TS over a 36T (ONIOM(HF/3-21g: UFF)) Quantum Cluster of Zeolite .....	54
4.2.2 (b)	Pathway 2: Methylation of Benzyl Alcohol with a Single TS over a 36T (ONIOM(HF/3-21g: UFF)) Quantum Cluster of Zeolite .....	59
4.2.3	Carboxymethylation of Benzyl Alcohol over a 36T (ONIOM(HF/3-21g: UFF)) Quantum Cluster of Zeolite ....	63
4.3	Comparison between the 3T (B3LYP/6-311G(d,p)) and 36T (ONIOM(HF/3-21G: UFF)) quantum clusters of zeolite .....	68
4.4	Reaction Mechanisms between Benzyl Alcohol and DMC over a 36T (ONIOM(B3LYP/6-31g(d,p): UFF)) Quantum Cluster of Zeolite .....	70

4.4.1	Adsorption of Reactants onto the Zeolite Surface over a 36T (ONIOM(B3LYP/6-31g(d,p): UFF)) Quantum Cluster of Zeolite .....	70
4.4.2	Methylation of Benzyl Alcohol over a 36T (ONIOM(B3LYP/6-31g(d,p): UFF)) Quantum Cluster of Zeolite .....	74
4.4.2 (a)	Pathway 1: Methylation of Benzyl Alcohol with Two TS over a 36T (ONIOM(B3LYP/6-31g(d,p): UFF)) Quantum Cluster of Zeolite .....	74
4.4.2 (b)	Pathway 2: Methylation of Benzyl Alcohol with a Single TS over a 36T (ONIOM(B3LYP/6-31g(d,p): UFF)) Quantum Cluster of Zeolite .....	79
4.4.3	Carboxymethylation of Benzyl Alcohol over a 36T (ONIOM(B3LYP/6-31g(d,p): UFF)) Quantum Cluster of Zeolite .....	82
4.5	Comparison between the 3T (B3LYP/6-31G(d,p)) and 36T (ONIOM(HF/3-21G: UFF) and ONIOM(B3LYP/6-31G(d,p): UFF)) Quantum Clusters of Zeolite .....	86
4.6	Comparison between the 36T ONIOM Methods with the DFT and HF Level of Calculation .....	89
4.7	Comparison between ONIOM Methods with the UFF and PM3 Level of Calculation .....	90
4.8	Rate Constant .....	92
 <b>CHAPTER V- CONCLUSIONS</b>		
5.1	Conclusions.....	95
5.2	Future Work and Recommendation.....	96
 <b>REFERENCES</b>		
<b>LIST OF PUBLICATIONS</b>		
		98
		112

## LIST OF TABLES

		<b>Page</b>
Table 4.1	The optimized bond parameters at the GS (GS1) and TS (TS1) over a 3T (B3LYP/6-31g(d,p)) quantum cluster of zeolite.	36
Table 4.2	The optimized bond parameters at the GSs (GS3 and GS4) and TSs (TS2 and TS3) over a 3T (B3LYP/6-31g(d,p)) quantum cluster of zeolite.	38
Table 4.3	The optimized bond parameters at the GS (GS5) and TS (TS4) over a 3T (B3LYP/6-31g(d,p)) quantum cluster of zeolite.	43
Table 4.4	The optimized bond parameters at the GSs (GS6 and GS7) and TS (TS5) over a 3T (B3LYP/6-31g(d,p)) quantum cluster of zeolite.	46
Table 4.5	The optimized bond parameters at the GS (GS1) and TS (TS1) over a 36T (ONIOM(HF/3-21g: UFF)) quantum cluster of zeolite.	53
Table 4.6	The optimized bond parameters at the GSs (GS3 and GS4) and TSs (TS2 and TS3) over a 36T (ONIOM(HF/3-21g: UFF)) quantum cluster of zeolite.	56
Table 4.7	The optimized bond parameters at the GS (GS5) and TS (TS4) over a 36T ONIOM(HF/3-21g: UFF) quantum cluster of zeolite.	61
Table 4.8	The optimized bond parameters at the GSs (GS6 and GS7) and TSs (TS5 and TS6) over a 36T (ONIOM(HF/3-21g: UFF)) quantum cluster of zeolite.	65
Table 4.9	The optimized bond parameters at the GS (GS1) and TS (TS1) over a 36T (ONIOM: (B3LYP/6-31G(d,p): UFF)) quantum cluster of zeolite.	73
Table 4.10	The optimized bond parameters at the GSs (GS3 and GS4) and TSs (TS2 and TS3) over a 36T (ONIOM: (B3LYP/6-31G(d,p): UFF)) quantum cluster of zeolite.	75
Table 4.11	The optimized bond parameters at the GS (GS5) and TS (TS4) over a 36T (ONIOM: (B3LYP/6-31G(d,p): UFF)) quantum cluster of zeolite.	80

		<b>Page</b>
Table 4.12	The optimized bond parameters at the GSs (GS6 and GS7) and TSs (TS6 and TS7) over a 36T (ONIOM: (B3LYP/6-31G(d,p): UFF)) quantum cluster of zeolite.	83
Table 4.13	The energy difference, $\Delta E$ , between the ONIOM methods performed with either the UFF or PM3 level of calculation.	91
Table 4.14	Kinetic parameters, after including Wigner's tunneling correction, for each TS of 3T and 36T quantum cluster of zeolite.	90

## LIST OF FIGURES

		<b>Page</b>
Figure 2.1	Distribution of Na <sup>+</sup> cations in different sites of faujasite framework.	14
Figure 2.2	The 36T quantum cluster of the faujasite framework.	16
Figure 2.3	The ONIOM model.	22
Figure 2.4	The ONIOM extrapolation scheme for (a) the two layered ONIOM method and (b) the three layered ONIOM method.	23
Figure 3.1	Clusters of the faujasite zeolite framework (a) 3T cluster model, (b) 36T of ONIOM model.	31
Figure 4.1	The adsorption structures of (a) benzyl alcohol and (b, c) dimethyl carbonate (DMC) at the zeolite surface.	33
Figure 4.2	The optimized GS (GS1) geometries with some important bond parameters (distances are reported in Å and angles are in degrees) of the reactants over a 3T (B3LYP/6-31g(d,p)) quantum cluster of zeolite.	35
Figure 4.3	The optimized TS (TS1) geometries with some important bond parameters (distances are reported in Å and angles are in degrees) of the reactants over a 3T (B3LYP/6-31g(d,p)) quantum cluster of zeolite.	36
Figure 4.4	Energy profile for the adsorption of reactants and the methylation reaction via Pathway 1, which involves two TSs (TS2 and TS3) over a 3T (B3LYP/6-31G(d,p)) quantum cluster of zeolite.	38
Figure 4.5	The optimized TS (TS2) geometries with hydrogen bond distances (Å) over a 3T (B3LYP/6-31G(d,p)) quantum cluster of zeolite.	40
Figure 4.6	The optimized TS (TS3) geometries with some important bond parameters (distances are reported in Å and angles are in degrees) of the reactants over a 3T (B3LYP/6-31G(d,p)) quantum cluster of zeolite.	42
Figure 4.7	The optimized TS (TS4) geometries hydrogen bond (Å) of the reactants over a 3T (B3LYP/6-31G(d,p)) quantum cluster of zeolite.	43

		<b>Page</b>
Figure 4.8	Energy profile for the adsorption of reactants and the methylation reaction via Pathway 2, which involves only a TS (TS4) over a 3T (B3LYP/6-31G(d,p)) quantum cluster of zeolite.	45
Figure 4.9	The optimized TS (TS5) geometries with hydrogen bond ( $\text{\AA}$ ) of the reactants over a 3T (B3LYP/6-31G(d,p)) quantum cluster of zeolite.	46
Figure 4.10	Energy profile for the adsorption of the reactants and the carboxymethylation reaction over a 3T (B3LYP/6-31G(d,p)) quantum cluster of zeolite.	48
Figure 4.11	The optimized geometries with some important bond parameters (distance is reported in $\text{\AA}$ and angle is in degrees) of the decarboxylation reaction (GS7) over a 3T (B3LYP/6-31G(d,p)) quantum cluster of zeolite.	49
Figure 4.12	The optimized GS (GS1) geometries with some important bond parameters (distances are reported in $\text{\AA}$ and angles are in degrees) of the reactants over a 36T (ONIOM(HF/3-21g: UFF)) quantum cluster of zeolite.	52
Figure 4.13	The optimized TS (TS1) geometries with some important bond parameters (distances are reported in $\text{\AA}$ and angles are in degrees) of the reactants over a 36T (ONIOM(HF/3-21g: UFF)) quantum cluster of zeolite.	53
Figure 4.14	Energy profile for the adsorption of reactants and the methylation reaction via Pathway 1, which involves two TSs (TS2 and TS3) over a 36T (ONIOM(HF/3-21G: UFF)) quantum cluster of zeolite.	55
Figure 4.15	The optimized TS (TS2) geometries with hydrogen bonds ( $\text{\AA}$ ) of the reactants over a 36T (B3LYP/6-31G(d,p)) quantum cluster of zeolite.	56
Figure 4.16	The optimized TS (TS3) geometries with some important bond parameters (distances are reported in $\text{\AA}$ and angles are in degrees) of the reactants over a 36T (ONIOM(HF/3-21G: UFF)) quantum cluster of zeolite.	59

		<b>Page</b>
Figure 4.17	The optimized TS (TS4) geometries with some important bond parameters (distance is reported in Å and angles are in degrees) of the reactants over a 36T (ONIOM(HF/3-21G: UFF)) quantum cluster of zeolite.	63
Figure 4.18	Energy profile for the adsorption of reactants and the methylation reaction via Pathway 2, which involves only a single TS (TS4) over a 36T (ONIOM(HF/3-21g:UFF)) quantum cluster of zeolite.	64
Figure 4.19	The optimized TS (TS5) geometries with some important bond parameters (distance is reported in Å and angle is in degrees) of the reactants over a 36T (ONIOM(HF/3-21G: UFF)) quantum cluster of zeolite.	65
Figure 4.20	Energy profile for the adsorption of reactants and the carboxymethylation reaction over a 36T (ONIOM(HF/3-21G: UFF)) quantum cluster of zeolite.	67
Figure 4.21	The optimized TS (TS6) geometries of the reactants over a 36T (ONIOM(HF/3-21G: UFF)) quantum cluster of zeolite.	68
Figure 4.22	The optimized GS (GS1) some important bond parameters (distances are reported in Å and angles are in degrees) of the reactants over a 36T (ONIOM: (B3LYP/6-31G(d,p): UFF)) quantum cluster of zeolite.	72
Figure 4.23	Energy profile for the adsorption of reactants and the methylation reaction via Pathway 1, which involves two TSs (TS2 and TS3) over a 36T (ONIOM: (B3LYP/6-31G(d,p): UFF)) quantum cluster of zeolite.	73
Figure 4.24	The optimized TS (TS1) geometries with some important bond parameters (distances are reported in Å and angles are in degrees) of the reactants over a 36T (ONIOM: (B3LYP/6-31G(d,p): UFF)) quantum cluster of zeolite.	75
Figure 4.25	The optimized TS (TS2) geometries with some important bond parameters (distance is reported in Å and angles are in degrees) of the reactants over a 36T (ONIOM: (B3LYP/6-31G(d,p): UFF)) quantum cluster of zeolite.	76

		<b>Page</b>
Figure 4.26	The optimized TS (TS3) geometries with hydrogen bonds (Å) of the reactants over a 36T (ONIOM: (B3LYP/6-31G(d,p): UFF)) quantum cluster of zeolite.	79
Figure 4.27	The optimized TS (TS4) geometries hydrogen bonds (Å) of the reactants over a 36T (ONIOM: (B3LYP/6-31G(d,p): UFF)) quantum cluster of zeolite.	82
Figure 4.28	Energy profile for the adsorption of reactants and the methylation reaction via Pathway 1, which only involves a single TS (TS4) over a 36T (ONIOM: (B3LYP/6-31G(d,p): UFF)) quantum cluster of zeolite.	83
Figure 4.29	The optimized TS (TS5) geometries with the hydrogen bond (Å) of the reactants over a 36T (ONIOM: (B3LYP/6-31G(d,p): UFF)) quantum cluster of zeolite.	85
Figure 4.30	Energy profile for the adsorption of reactants and the carboxymethylation over a 36T (ONIOM: (B3LYP/6-31G(d,p): UFF)) quantum cluster of zeolite.	86
Figure 4.31	The optimized TS (TS6) geometries with some important bond angles (degrees) of the reactants over a 36T (ONIOM: (B3LYP/6-31G(d,p): UFF)) quantum cluster of zeolite.	87
Figure 4.32	The overall energy profile for the adsorption of reactants and methylation reaction via Pathway 1, which involves two TS (TS2 and TS3) based on 3T and 36T quantum cluster .	88
Figure 4.33	The overall energy profile for the adsorption of reactants and methylation reaction via Pathway 2, which involves only a TS (TS4) based on 3T and 36T quantum cluster.	89
Figure 4.34	The overall energy profile for the adsorption of reactants and carboxymethylation reaction based on 3T and 36T quantum cluster.	90

## LIST OF ABBREVIATIONS

AM1	Austin model 1
B3LYP	Becke three parameter Lee, Yang, and Parr exchange-correlation functional
BME	Benzyl methyl ether
BME	Benzyl methyl carbonate
D6R	Double six ring
DFT	Density functional theory
DMC	Dimethyl carbonate
DMN	Dimethylnaphthalene
EFSA	European Food Safety Authority
GB	Giga-bytes
GS	Ground state
GSE	Sun Grid Engine
GTO	Gaussian type orbitals
HF	Hartree–Fock
IRC	Intrinsic reaction coordinate
MM	Molecular mechanics
MNDO	Modified intermediate neglect of differential overlap
MP	Moller-Plesset Perturbation Theory
MTBE	Methyl tert-butyl ether
NaX	X-Faujasite
NaY	Y-Faujasite
ONIOM	Our own <i>n</i> -layered integrated molecular orbital and molecular mechanics
PM3	Parametric method number 3
QM	Quantum mechanics
RAM	Random access memory
S <sub>N</sub> 2	Bimolecular nucleophilic substitution
STO	Slater type orbitals
TS	Transition state
TST	Transition state theory

UFF      Universal force field  
USM      University Sains Malaysia

## LIST OF SYMBOLS

$K$	Rate constant
$E_a$	Activation energy
$h_p$	Plank's constant
$k_B$	Boltzmann's constant
$N_A$	Avogadro's constant
$\text{NO}_x$	Nitrogen oxides
$Q_A$	Partition functions for the reactants
$Q_{TS}$	Partition functions for the transition state structure
$T$	Temperature
$\Gamma$	Wigner's tunneling correction
$\rho$	Electron density

## ABSTRAK

Sebatian benzil metil eter (BME) kebanyakannya disintesis oleh industri kimia sebagai bahan permulaan bagi sintesis sebatian lain. Untuk mencapai matlamat kimia hijau, BME boleh disintesis daripada benzil alkohol dan dimetil karbonat (DMC) menggunakan pemangkin zeolit. DMC adalah agen pemetilan dan agen pengkarboksimetilan yang kurang toksik berbanding dengan agen yang lain. Tujuan kajian ini ialah untuk mengkaji mekanisme tindak balas yang berkemungkinan bagi tindak balas benzil alkohol dan DMC dengan pemangkin zeolit. Tindak balas pemetilan dan pengkarboksimetilan benzil alkohol dikaji menggunakan dua rangka kerja zeolit gugus iaitu: gugusan kuantum 3T bagi zeolite yang diperhitungkan dalam teori ketumpatan fungsian (DFT) dan rangka kerja lanjutan 36T yang dikaji dengan pendekatan ONIOM menggunakan Hartree-Fock (HF) dan DFT yang terbenam dengan mekanik molekul UFF dan kaedah semiempirik PM3. Kedua-dua rangka kerja menunjukkan tindak balas pemetilan adalah lebih utama secara kinetik berbanding dengan tindak balas pengkarboksimetilan. Terdapat dua laluan yang dijumpai bagi tindak balas pemetilan, pertama melibatkan dua keadaan peralihan (TS) dan yang kedua hanya mempunyai satu TS. Pemetilan melalui laluan dua-TS didapati lebih diutamakan secara kinetik berbanding dengan laluan tunggal TS. Dalam catatan, ONIOM(DFT:UFF) dan ONIOM(DFT:PM3) menunjukkan keputusan yang sama. ONIOM(HF:UFF) telah menunjukkan struktur yang dioptimumkan yang sama berbanding dengan ONIOM(DFT:UFF) dan tenaga lebih anggar. Pemalar kadar bagi tindak balas yang dikaji adalah dikira menggunakan teori keadaan peralihan dan langkah penentuan kadar telah ditentukan.

## ABSTRACT

Benzyl methyl ether (BME) compounds are largely synthesized by the chemical industry for use as a starting material for the synthesis of other organic compounds. In order to achieve the target of green chemistry, BME can be synthesized from benzyl alcohol and dimethyl carbonate (DMC) using a zeolite catalyst. DMC is a good methylating and carboxymethylating agents that is, in contrast to other such agents, a relatively non-toxic compound. The target of this study is to investigate the possible reaction mechanisms for the reaction of benzyl alcohol and DMC over the zeolite catalyst. In this study, the methylation and carboxymethylation reactions of benzyl alcohol over a 3T quantum cluster of zeolite was investigated by density functional theory (DFT). A 36T extended framework was investigated by the ONIOM approach, with Hartree-Fock (HF), DFT, and embedded with the UFF molecular mechanic and PM3 semiempirical approach. Both frameworks revealed two pathways for the methylation reaction, the first involving two transition states (TSs) and the second only a single TS. Methylation via the two-TS pathway was found to be kinetically more stable than the single-TS pathway whilst the methylation reaction was kinetically favored over the carboxymethylation reaction. The ONIOM(DFT:UFF) and ONIOM(DFT:PM3) have shown similar results, while the ONIOM(HF:UFF) has shown similar optimized structures and overestimated energies. The rate constant for the studied reactions were calculated by using the transition state theory and the rate determining step was determined.

## CHAPTER I

### INTRODUCTION

#### 1.1 Introduction

Benzyl methyl ether (BME) is an asymmetrical ether (Wade, 2006) that exists naturally in spices, herbs, mints, dried fish products, mushroom, tea, juices and alcoholic beverages and is also added to food as a flavoring agent due to its pleasant fruity odor (Aguilar et al., 2008). Currently, there is no evidence (e.g. toxicity studies) to show that the consumption of BME at less than 540 microgram per person per day will cause any negative effect on human daily metabolism (Aguilar et al., 2008).

In addition to the food industry, BME is also used as a solvent for organic compounds, a starting material for the synthesis of other organic compounds (Grützmaier & Dohmeier-Fischer, 1998) and as a booster for gasoline combustion (Chen et al., 2009; Ma et al., 2007). For instance, Grützmaier et al. (1998) have used BME instead of vinyl ether as a starting material to react with benzyl cation to produce a four unit of homopolymer.

Ma et al. (2007) suggested BME would be a good substitute for methyl tert-butyl ether (MTBE) in order to enhance gasoline combustion. MTBE is an additive to gasoline to increase the octane number and to avoid air pollution caused by elimination of toxic gases such as carbon monoxide (Chen et al., 2009; Kolb & Püttmann, 2006). MTBE is colorless (Juhler & Felding, 2003), has high solubility in water (Centi et al., 2002; Chen et al., 2009), high mobility, resists to biodegradation (Centi et al., 2002) and gives unpleasant odour to water even at very low



allow a complete reaction to occur. As a result, the same amount of inorganic salt is produced that needs to be discarded as waste (Selva, 2007; Tundo et al., 2004).

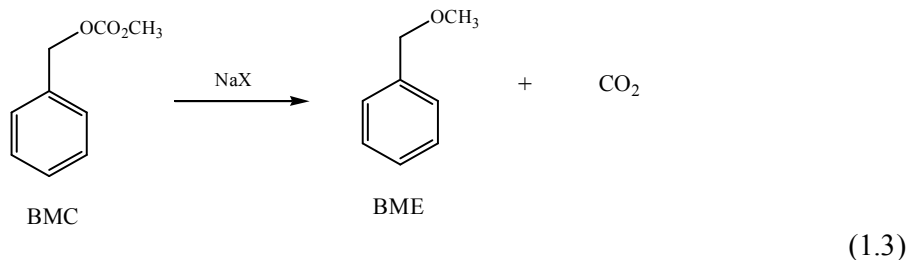
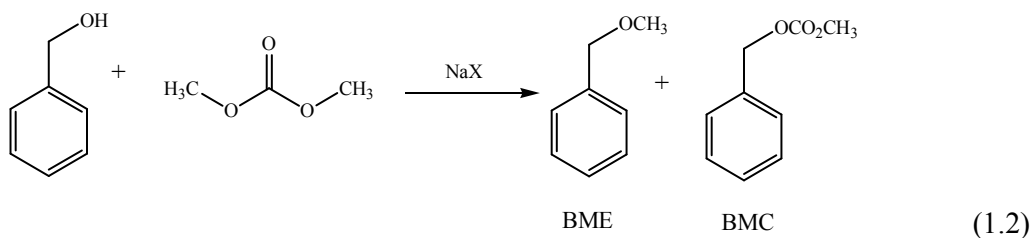
In order to achieve the target of green production of BME, Ma et al and co-workers have reviewed the synthesis of BME by using methanol and toluene in electrochemical catalytic reactor (Chen et al., 2009; Chen et al., 2008; Chen et al., 2007; Ma et al., 2007). They found that the electrolyte system with  $\text{SO}_4^{2-}/\text{ZrO}_2$  or  $\text{Fe}_2\text{O}_3\text{-MoO}_3\text{-P}_2\text{O}_5$  salt catalyst give a high selectivity to BME, up to 75% of percentage yield (Chen et al., 2007; Ma et al., 2007). However, this method of synthesis usually give one or more side product due to the presence of toluene and methanol free radicals continuously react with other intermediates and leads to undesired by products were formed at the same time.

The experimental studies on green synthesis of methyl ethers with nucleophile (alcohol) and dimethyl carbonate (DMC) over an acidic or basic catalyst have been extensively reported (Selva et al., 2008; Selva, 2007; Tundo et al., 2004; Tundo & Selva, 2002; Tundo, 2001). Synthesis of BME with nanostructured catalysts, X-faujasites (NaX) and Y-faujasites (NaY), gave more than 90% product yield. Furthermore, when the temperature is raised, the reaction takes place faster with the NaX catalyst than with the NaY catalyst (Tundo et al., 2004).

DMC is a non-toxic alkylating agent (Shaikh et al., 1996) that can be used to replace alkyl halides for less harmful methylation and carboxymethylation reactions. The advantages of DMC are that (i) no extra solvent is necessary because DMC is a good solvent for many organic compounds, (ii) the reaction is only slightly or not at

all exothermic, and (iii) it does not lead to the production of harmful solid wastes, with methanol and carbon dioxide being the only side products which can easily be disposed off (Selva, 2007; Tundo & Selva, 2002).

DMC behaves as a carboxymethylating agent at low reaction temperature (90 °C) and carboxymethylation reaction predominates (Tundo & Selva, 2002; Tundo, 2001). In contrast, at 160 °C, DMC behaves as a methylating agent and methylation reaction predominates (Tundo & Selva, 2002; Tundo, 2001). However, Selva et al. (2008) reported that the faujasite zeolite catalyst allows both methylation and carboxymethylation reactions to occur simultaneously at 165 – 168 °C (Selva et al. 2008). Thus, the two main possible products formed are benzyl methyl carbonate (BMC) and BME, as shown in Equation 1.2. Moreover, as the temperature is increased to 200 °C, BMC will undergo decarboxylation to form BME (Selva et al., 2008), as shown in Equations 1.3.



Even though experimental studies have shown that BMC can be synthesized using benzyl alcohol and DMC over zeolite, the actual reaction mechanisms involved still remain unclear (Selva, 2007). In order to predict the reaction mechanism in a

zeolite catalyst system, theoretical studies can be utilized to provide a better understanding for the complicated chemical reactions which are otherwise not possible to evaluate by experimental investigations alone (Bobuatong & Limtrakul, 2003; Kasuriya et al., 2003; Namuangruk et al., 2004; Rungsirisakun et al., 2005; Sun et al., 2010; Wongthong et al., 2004).

Computational chemistry implements the theories of quantum mechanics (QM) and molecular mechanics (MM) (Holme, 2010; Subramanian, 1997). The QM method is an accurate and expensive ab initio method, while the MM method is a cheap method which performs much faster compared to the QM method. However, simple classical parameter is applied in the MM method, therefore it does not produce results as reliable as the QM method. Zeolites usually have several hundreds of atoms per unit cell (Bobuatong & Limtrakul, 2003; Namuangruk et al., 2004; Nie et al., 2011; Rungsirisakun et al., 2005; Sun et al., 2010; Wongthong et al., 2004) and studies of reaction mechanisms over a zeolite system fully based on either QM or MM method is not encouraged. This is due to the fact that QM method is very time consuming, computationally expensive and impractical, meanwhile, the MM method does not produce results as reliable as the QM method.

Many theoretical studies have been carried out on chemical reactions over the zeolite (Namuangruk et al., 2004; Nie et al., 2011; Rattanasumrit, 2005; Solans-Monfort et al., 2002; Sun et al., 2010;) or the biological systems (Lundberg & Morokuma, 2009; Vreven & Morokuma, 2006) which involves hundreds to thousands of atoms based on quantum mechanics/molecular mechanics (QM/MM) hybrid method. Only the reacting region is treated by an accurate QM method and

the extended environment is treated by MM method. These studies have concluded that the QM/MM method is practical and the results are satisfactory (Namuangruk et al., 2004; Vreven & Morokuma, 2006). Therefore, the interest of this study was to investigate the reaction mechanisms involved in BME production from benzyl alcohol and DMC over a NaX zeolite catalyst. From an industrial prospective, understanding the reaction mechanisms and pathway will provide a better foundation for optimizing the reaction conditions in order to achieve a more efficient, and so economically and environmentally viable process (Namuangruk et al., 2004).

## **1.2 Problem Statement**

BME can be produced by reaction of benzyl alcohol with DMC over faujasite zeolite with 100% conversion rate (Selva et al., 2008). However, the interaction mechanisms and the pathways of the reaction is still debatable. This study therefore, attempts to elucidate the reaction mechanisms for the methylation and carboxymethylation reactions using theoretical approach applying a hybrid QM/MM method. There are no reports of the theoretical studies on the interaction energies between the complex and zeolite, the adsorption structures of the complexes in their transition state (TS) and the final products, and reaction mechanisms for the methylation and carboxymethylation reactions.

## **1.3 Significant of Research**

BME compounds are largely synthesized by the industries to be used as a starting material to synthesize other organic compounds. However, there is no experimental data reported for the methylation and carboxymethylation reactions with respect to the energy profile. By using computational simulation, we can predict

the energy profile of stepwise reaction mechanism in a more effective way by reducing the use of chemicals, experimental time and cost. Also, we can deduce the best conformation of the complexes with the zeolite in order to optimize the production of desire products. Moreover, reaction mechanisms will be investigated for the methylation and carboxymethylation reactions which are still open for proposal.

#### **1.4 Objectives**

The objectives of the calculations for the reaction mechanism between benzyl alcohol and DMC are as follows: (i) to predict the optimized geometries of the different complexes in the TS and ground state (GS) over a small (3T) or an extended (36T) quantum cluster of zeolite, ii) to calculate the energy profile for methylation and carboxymethylation reactions, (iii) to investigate the possible reaction mechanisms for the reaction of benzyl alcohol and DMC over a zeolite catalyst, (iv) to compare the reaction mechanisms and energy profile of the reactants over a 3T or a 36T quantum cluster of zeolite, and (v) to compare the results of the 36T of zeolite with different types of QM/MM methods.

#### **1.5 Scope of Study**

In this study, the 3T and extended 36T of faujasite zeolite framework were used. The crystal structure of zeolite was built according to the NaX crystal structure proposed by Olson (1995). Calculations were performed using Gaussian 03 software under Linux operating system. GaussView 03 and Chemcraft softwares were the visualizing tools for viewing the geometry of molecules, vibrational frequencies and intrinsic reaction coordinate (IRC) pathways.

## CHAPTER II

### LITERATURE REVIEW

#### 2.1 Introduction to Zeolite

The first natural zeolite was discovered more than 200 years ago by Freiherr Axel Fredrick Cronsted, a Swedish mineralogist (Roque-Malherbe, 2001; Xu et al., 2007). The microporous crystalline aluminosilicates now known as zeolites, comprised of  $TO_4$  units, where T is either Si or Al atoms. The pure silicate zeolite framework is neutral (Kaduk & Faber 1995). With the substitution of aluminium atom in place of tetrahedrally coordinated Si atoms will give a negative charge on the framework, which is usually balanced by cation from group I and II (Gauthier et al., 1988; Kaduk & Faber 1995; Sillar & Burk 2002). The  $SiO_4$  and  $AlO_4$  tetrahedra are linked to each into a 3-dimensional framework (Gauthier et al., 1988; Kaduk & Faber 1995; Sillar & Burk 2002; Xu et al., 2007). The connectivity of  $SiO_4$  and  $AlO_4$  tetrahedra is not random. On the other hand, it strictly obeys the Löwenstein's rule.

The Löwenstein's rule states that two units of  $TO_4$  are connected with oxygen, only one of the  $TO_4$ 's center is allowed to substitute Al atom. Next, when two units of  $AlO_4$  are adjacent to one another, either of the  $AlO_4$  unit must achieve coordination number which is larger than four (Szostak, 1989). Generally speaking, the arrangement of two adjacent  $AlO_4$  tetrahedral is forbidden but only one aluminium atom is allowed to bond with four neighboring Si atoms (Dann et al., 1996; Xu et al., 2007). Ab initio studies of the Al–O–Al linkages by Tossell (1993) also demonstrated that the two alternating isomer of Si–O–Al–O–Si–O–Al is much more stable than the paired Si–O–Si–O–Al–O–Al linkage.

In the early years, due to the lack of technology, these zeolite were poorly characterized. Impurities existed in natural zeolites, and with expensive transportation cost and many other reasons made natural zeolites not to meet the huge demand of the industries (Roque-Malherbe, 2001). As a result, research on the synthesis of zeolite became one of the main interest of material scientists by mimicking the geothermal conditions of natural zeolite formation (Xu et al., 2007).

In the 1940's, the first zeolite was successfully synthesized and this was followed by various types of zeolite X and Y (Xu et al., 2007). Zeolite X is known as a low silica zeolite or aluminum rich zeolite with molar ratio of Si/Al approximately equal to one. The maximum number of possible aluminium content present in the zeolite framework is strictly following Löwenstein's Rule. Thus, zeolite X has a higher number of cation exchange sites (Beagley et al., 1985; Flanigen, 1980) and the surface is highly selective for polar molecules (Flanigen, 1980). In contrast, zeolite Y has higher silica content than aluminum with molar ratio of Si/Al ranged from 1.5 – 3.0 (Flanigen, 1980; Gleeson & Limtrakul, 2007) resulting in a hydrophobic surface (Flanigen, 1980). Chen (1976) also reported the dealuminized mordenite sample with high silica content had hydrophobic or a non-polar surface.

## **2.2 Applications of Zeolite**

In the early stage, with the knowledge that natural zeolite exhibits water-adsorption ability, scientists had extensively applied this material as adsorbents and desiccants. Traditionally, zeolites are widely applied in gas drying (Lee, 1973), catalysis (Li et al., 2011; Lee, 1973; Vadrine, 1985), and pollution control (Li et al.,

2011; Lee, 1973; Panagiotis, 2011). Later on, the applications of natural zeolites were expanded to separation and purification (Xu et al., 2007).

In the early days, many reports reviewed that the zeolite as an impressive catalyst for cracking of hydrocarbon polymers into smaller molecules (Rajagopalan & Young 1988; Vadrine, 1985), alkylation of aromatic compounds, isomerization reactions (Vadrine, 1985) and conversion of low molecular weight hydrocarbons to high molecular weight hydrocarbons (Garwood, 1983; Vadrine, 1985). The synthetic ZSM-5 zeolite was discovered to be very effective in the conversion of methanol gasoline with high octane number (Vadrine, 1985). It was used successfully to convert the low molecular weight olefins ( $C_2 - C_{10}$ ) to high molecular weight oligomers (more than  $C_{30}$ ) using ZSM-5 zeolite as the catalyst (Garwood, 1983). Besides that, Lee (1973) reported that the removal of water from petrochemical raw material is the most prominent step in the pre-separation of ethylene and propylene. The hydrophilic surface of zeolite adsorbed the water molecules on the zeolite surface effectively.

Moreover, zeolite X and Y were discovered to exhibit great catalytic properties in the cracking of hydrocarbon. The presence of Brønsted or Lewis acid properties (Flanigen, 1980; Vadrine, 1985), made it possible to prepare multivalent exchangeable metal cation forms of zeolites (Flanigen, 1980; Lee, 1973; Vadrine, 1985). Furthermore, the rapid developments of zeolite in catalysis application are due to the very strong adsorption forces within zeolites (Flanigen, 1980). The zeolites also exhibit shape selective properties, where the uniform pore size is able to control the diffusion rate of reactants and products (Vadrine, 1985). Thus, zeolite has the

ability to concentrate the reactant and allows bimolecular reactions to occur and give a high percentage of yields (Flanigen, 1980; Vedrine, 1985). The stability of zeolite in terms of chemical (Lee, 1973) and hydrothermal (Lee, 1973; Wernert et al., 2005) makes it a much favored material in separation, purification of compounds and many other applications.

Zeolites have also contributed immensely in solving environmental issues such as removal of heavy metals in soils, reduction of heavy metals in gasoline (Panagiotis, 2011), purification of waste water, drinking water (Li et al., 2011; Panagiotis, 2011), toxic gases (Lee, 1973; Marcus & Cormier, 2000) and removal of industrial hazardous nuclear waste (Malekpour et al., 2008; Panagiotis, 2011). Water is considered polluted when there are chemical, biological contaminants resulting in physical changes, which bring destructive effects to the living organisms. Underground water which is also the water supply in man's daily life might contain nitrate ( $\text{NO}_3^-$ ) or phosphate ( $\text{PO}_4^{3-}$ ) ions. The contaminated water resources are frequently observed in regions that are near agricultural areas due to improper sewage disposal. These contaminants are carcinogenic and may cause fatality in infants and adults (Miller & Spoolman, 2009). The major air pollutants currently damaging earth are carbon monoxide, nitrogen oxides ( $\text{NO}_x$ ), sulphur dioxide, sulphuric acid and volatile organic compounds (Miller & Spoolman, 2009). The hydrophobic property of zeolite is also highly effective towards removal of these gases (Marcus & Cormier, 2000).

Interestingly, in recent years, these microporous materials have been used in the biomedical field (Bonferoni et al., 2007; Cerri et al., 2004; Pavelic et al., 2001;

Wernert et al., 2005). Cerri et al. (2004) reported that the clinoptilolite, a natural zeolite with zinc metal ion is able to be combined with an antibiotic to treat dermatology problem such as anti acne. However, research on optimization of the zeolite system need to be carried out further in order to enhance the medication formulation (Bonferoni et al., 2007). Besides, Wernert et al. (2005) suggested that zeolite is can be used to adsorb the uremic toxins released by kidney. The large pore size of zeolite allows the low molecular weight protein to pass through and adsorb in it.

Nowadays, China has extensively used zeolite as one of the construction materials (Feng & Peng, 2005) where it is mixed with the cement to manufacture concrete with higher stability (Feng et al., 1979 as cited in Feng & Peng, 2005). Zeolite with silver ion is a good material in making bricks, cement and other construction material because it is known to exhibit anti bacterial properties. In addition, it is hard, able to decrease permeability of concrete, resistance to alkali-aggregate reaction and avoid concrete from spalling (Feng & Peng, 2005).

### **2.3 The Faujasite Zeolite Framework**

Zeolite X and Y of faujasite share the same structural framework (Bein, 1992). The only difference is the Si/Al ratio, where zeolite X usually contains 88 cations per unit cell (Bein, 1992, Olson, 1995); while zeolite Y contains approximately 56 to zero cation per unit cell (Kaduk & Faber, 1995). The solidate cage and hexagonal prism are the composite building units of faujasite zeolite framework. The sodalite cages are connected through four double six ring (D6R)

with a diameter of supercage with 12 Å. The supercages are linked through the 12 ring windows to give a diameter of 7.4 Å (Kaduk & Faber, 1995; Bein, 1992).

The Na<sup>+</sup> cations are found distributed in four different sites of the faujasite zeolite. Figure 2.1 shows the faujasite zeolite structure with the possible locations of Na<sup>+</sup> cations.

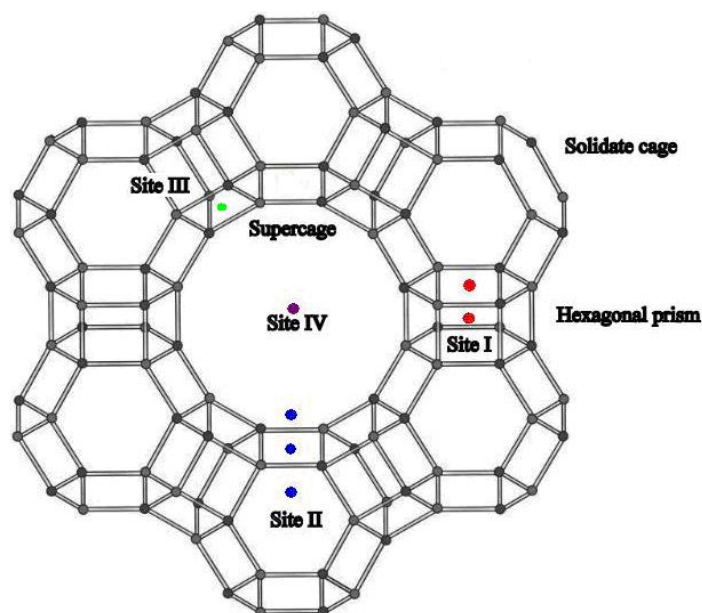


**Figure 2.1:** Distribution of Na<sup>+</sup> cations in different sites of faujasite framework (Kaduk & Faber, 1995).

At the site I, the cations are found in the center of hexagonal prisms which are connected to the sodalite cages, cations at site II are observed in the supercages or center of the hexagonal window of the sodalite cages, cations at the site III are located in the supercages of the square window and cations at the site IV are observed at the center of the supercages (Frising & Leflaive, 2008; Jaramillo & Auerbach, 1999; Kaduk & Faber, 1995; Xu et al., 2007).

Previous experimental and theoretical studies have characterized the crystal structure of faujasite zeolite framework by the X-ray diffraction (XRD) (Olson, 1995), nuclear magnetic resonance (NMR) simulation (Feuerstein et al., 1996; Melchior et al., 1982), and molecular dynamics with computer graphic techniques (Himei et al., 1996). According to Frising and Leflaive (2008), the distribution of  $\text{Na}^+$  cations can be found in several active sites of the NaX zeolite in order to maximize their interaction with neighbouring oxygen atoms and to diminish the electrostatic repulsion resulting from the  $\text{Na}^+$  cations. However, small molecules such as water molecules can pass through the solidate cages easily and the polar molecules will attract more cations to the supercages. Thus, there will be high occupancies of  $\text{Na}^+$  cations at site II and III.

In this study, we have modelled the position of  $\text{Na}^+$  cation at site II, which is in the supercage, as shown in Figure 2.2. This is due to the fact that benzyl alcohol and DMC are big molecules and they are only able to pass through the supercages large pore size (12 Å diameters), adsorb on to the zeolite surface and react with one another. The modeled  $\text{Na}^+$  ion did not bind with a particular oxygen atom of  $[\text{AlO}_4]^-$  tetrahedron, but it symmetrically connected to the two oxygen atoms (O1 and O2) of  $[\text{AlO}_4]^-$  and this structure has been confirmed by an ESR experiment (Hosono et al., 1982 as cited in Bobuatong & Limtrakul, 2003).

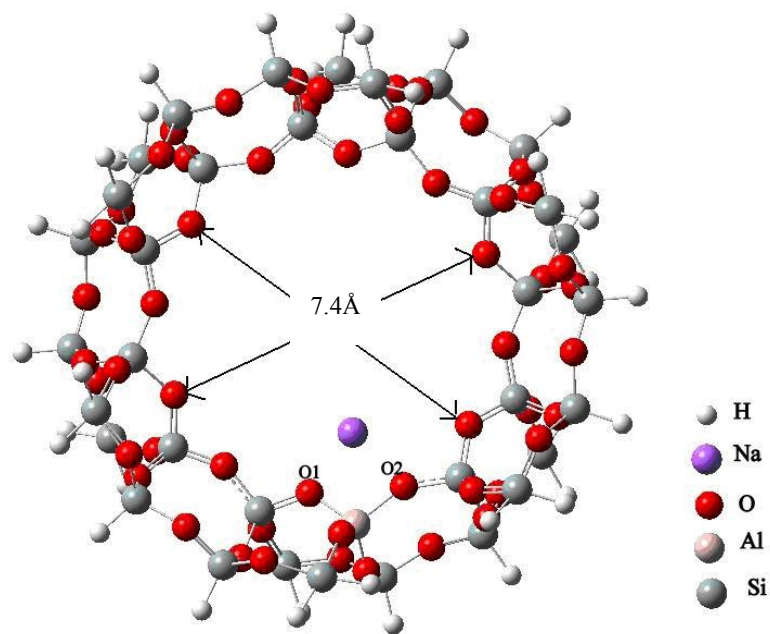


**Figure 2.2:** The 36T quantum cluster of the faujasite framework.

## 2.4 Introduction of Computational Chemistry

The importance of computational methods is arising in the physical chemistry field (Roseanne, 2007) due to the development of powerful supercomputers (da Silva & Svendsen, 2007; Walker et al., 1981). The attention of computational chemistry is the combination of mathematical equations with computing skills to resolve a complicated chemistry problem (Meldrum, 1955). First of all, the molecular electronic structures and molecular interactions are converted into numerical and their properties are calculated by the quantum and classical physics equations (Eliav, 2008; da Silva & Svendsen, 2007). However, when the number of electrons in the system increases, the calculations will become more and more complicated and time consuming (da Silva & Svendsen, 2007; Mammino, 2006). Hence, assumptions are necessary to be made (Mammino, 2006) to simplify the calculations and speed up the time of calculations.

Nowadays, the theoretical chemistry is not only often used to support the experimental results (Mammino, 2006) but could also make accurate predictions for the occurrence of chemical reactions before experimental work is carried out (Eliav, 2008; Pearson et al., 1977). It is also very helpful to develop 3D model of complexes, predict molecular geometries and spectroscopy properties (da Silva & Svendsen, 2007; Walker et al., 1981), study the reaction mechanisms (da Silva & Svendsen, 2007; Mohr, 2006), calculate the physical properties and examine compounds which are rarely found or compounds that have yet successfully synthesized (Eliav, 2008).

Computer is widely applied in the chemistry calculations due to many good qualities provided by the computer simulations compared to the conventional experimental methods. The computer can perform operations faster, process various types of information simultaneously and save plenty of cost and time. Also, the computer allows the investigation of large and realistic systems (Mohr, 2006), such as the zeolite, proteins and enzymatic systems. In addition, computer simulations experience a lower error rate such as systematical error which often occurs in experimental work.

#### **2.4.1 Ab-initio Methods**

The ab-initio methods are predicted mathematically based on Schrödinger's equation (Luo, 2010) by using the speed of light, Planck's constant and masses of the electrons and nuclei (Meller, 2001). The Hartree–Fock (HF) method is a common ab-initio method to calculate the molecular wave function (Young, 2002; Levine, 2000). Hartree approximation assumes each electron is not interacting with other electrons and the approximate wave function is the  $n$ -electron wave function with a product of

$n$  one-electron wave functions (Atkins & Paula 2006; Argaman & Makov 2000). In order to include the spin and the Pauli Exclusion Principle, Fock pointed out that the anti-symmetric product of spin-orbital must be taken into account to improve the approximate wave function (Levine, 2000). In general, the HF method uses the simplified one-electron equations, where every one-electron equation is solved to obtain a wave function (Young, 2002). The HF method has produced reliable results in terms of the optimized geometries, inter atomic distances, bond angles and vibrational frequencies with the reference of experimental data. However, the values of the total energies are below satisfactory even when a large basis set is applied in the calculations (Marshall, 2008).

Meanwhile, the density functional theory (DFT) is another method which is highly implemented in the ab-initio calculations (Drut et al., 2010; Jensen, 2007; Young, 2002) to predict the structure of atoms, molecules, crystals, surfaces, and their interactions (Jensen, 2007). The aim of the DFT method is to calculate the electron density,  $\rho$  rather than the molecular wave function (Levine, 2000; Atkins & Paula 2006; Drut et al., 2010; Young, 2002). The electron density determines the external potential for the electronic system and minimizes the total energy of the system (Meller, 2001). The Coulomb repulsion integral of DFT method is only calculated once over the electron density and the calculation is rather faster than the HF method (Drut et al., 2010). The DFT method such as B3LYP/6-31G(d) is very reputable in computational accuracy without requirement of additional computing time and it is considered as a standard model that can be implemented to many chemistry applications (Drut et al., 2010). Also, DFT calculations are reasonable to employ in large system with many electrons and it is much accurate compared to the

results obtained from HF method (Drut et al., 2010). However, the main drawback of ab-initio method is it is computationally expensive, time consuming (Young, 2002) and the time of calculation highly depends on the method of calculation (da Silva & Svendsen, 2007).

#### **2.4.2 Semi-empirical Methods**

The semi-empirical method applies the same concept as the ab-initio, HF method. However, the semi-empirical methods are simplified, with only the valence electrons are taken into account but the core electrons are not considered in order to speed up the time of calculations (Jensen, 2007; Hehre, 2003; Thiel 2000). Several examples of semi-empirical methods are the Austin model 1 (AM1) (Dewar et al., 1985), parametric method number 3 (PM3) (Rzepa & Yi, 1991) and modified intermediate neglect of differential overlap (MNDO) (Dewar & Li, 1974). These methods neglected many smaller electron repulsion integrals and the remaining integrals are standardized with parameters to fit the experimental data (Jensen, 2007; Levine, 2000).

One of the limitations of the semi-empirical methods is that they are only suitable for systems which have been parameterized with reliable experimental data (Jensen, 2007; Thiel 2000) but they are not able to predict the complexes of transition metals (Jensen, 2007). Semi-empirical methods give reliable results in the prediction of geometries, as well as the geometries of the first row transition metal compounds (Hehre, 2003). However, no polarizability data are applied in semi-empirical model (Jensen, 2007) and this model is not suitable for thermochemical calculations (Hehre, 2003).

### 2.4.3 Molecular Mechanics Methods

Molecular mechanics (MM) are simple, fast and accurate computational methods which used classical parameterization of molecule (Boeyens & Comba, 2001; Rogers 1998). MM methods of calculation did not involve the wave function or electron density (Levine, 2000), whereas it used simple rules with reduced parameters sets to predict the force field parameters. These parameters are based on the molecule bond stretching ( $E_{\text{stretch}}$ ), bond bending ( $E_{\text{bend}}$ ), torsional and inversion barriers ( $E_{\text{tor}}$ ), van der Waals interactions ( $E_{\text{vdw}}$ ), electrostatics interactions ( $E_{\text{dd}}$ ) and other related structural parameters. The total energy for the conformation of a molecule is expressed as in Equation 2.1 (Jensen, 2007; Levine, 2000; Rogers, 1998; Rappié et al., 1992; Duchamp, 1979).

$$V = \sum E_{\text{stretch}} + \sum E_{\text{bend}} + \sum E_{\text{tor}} + \sum E_{\text{vdw}} + \sum E_{\text{dd}} \dots \quad (2.1)$$

Systems with over hundreds of atoms are impractical to use ab initio methods for calculation. Therefore, MM methods can be applied in the non reacting part of biochemistry, molecular biology, pharmacology and zeolite systems in order to fasten the calculations (Rogers, 1998). Universal force field (UFF) is one of the MM methods which often embedded with the quantum mechanics method to simplify the calculations of big systems (Levine, 2000) and optimizations of systems with more than thousand of atoms can be achieved with low computational costs (Jensen, 2007).

Nevertheless, with the implementation of general parameterized force field, we could not expect MM methods to produce good quality of results but predictions of geometries are often comparable with the experimental values (Jensen, 2007; Levine, 2000). The MM methods only yield good results for compounds with good

parameters and available information. In contrast, for those new or strange molecules which did not have parameterized force field, the MM methods are not able to predict the geometries correctly (Jensen, 2007; Hehre, 2003). Moreover, the MM methods cannot be used to study the reaction mechanisms due to the calculation methods do not involve electron density of molecules, which is crucial in chemical reaction studies (Hehre, 2003). In general, the MM methods are said to be reliable if the results are compatible with the experimental data (Jensen, 2007).

#### **2.4.4 Quantum Mechanics/Molecular Mechanics (QM/MM) Methods**

ONIOM (our own *n*-layered integrated molecular orbital and molecular mechanics) is a method which embedded the QM and MM methods. The QM methods are derived from the classical mechanics which used the Schrödinger equation to describe the motion of a particle (Melchior et al., 1982). The QM involves ab initio calculations such as Hartree-Fock (HF), Density Functional Theory (DFT) and Moller-Plesset Perturbation Theory (MP2, MP3, etc.) (Feuerstein et al., 1996). However, the MM methods are unlike the QM methods, where they are based on the classical mechanics law of motion and only consider the molecule as group of particles (atoms) that carry masses (Melchior et al., 1982).

The ONIOM model can be visualized as an onion with multilayer of skin and is shown in Figure 2.3 (Morokuma, 2003).

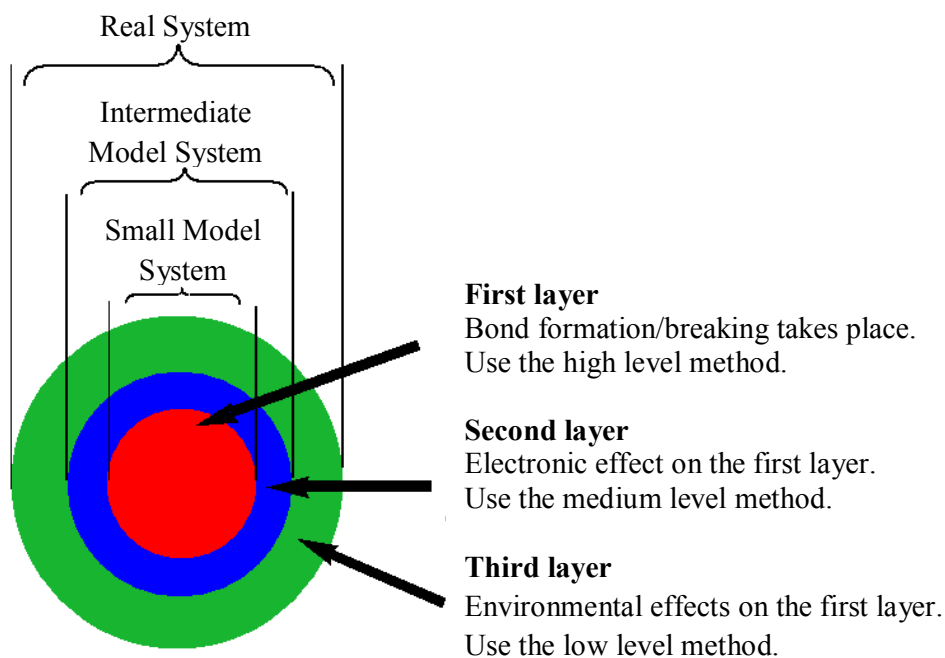


**Figure 2.3:** The ONIOM model (Morokuma, 2003).

ONIOM methods apply high level of theory at the specific region where reaction takes place where this region is identified as QM region and the remaining supporting system is treated at lower level of theory and is identified as MM region (Cornell et al., 1995; Frising & Leflaive, 2008; Kong et al., 2000). The ‘high’ and ‘low’ denotes the expensive and inexpensive method which is applied in the calculations, respectively (Lundberg & Morokuma, 2009; Vreven & Morokuma, 2006). The target of ONIOM calculation is to treat the large real system at high level of calculation,  $E(\text{real,high})$ . By this method, we could estimate the energy of real system with a low level method of calculation,  $E(\text{real,low})$  and also apply an accurate high level calculation to a smaller model system,  $E(\text{model,high})$  (Morokuma, 2003). The ‘model’ denotes the model system which corresponds to the real system and the ‘real’ denotes the model system which contains all of the atoms in the system and is calculated at MM level. (Morokuma, 2003).

Figure 2.4 shows the ONIOM extrapolation scheme for a molecular system partitioned into two and three layers.

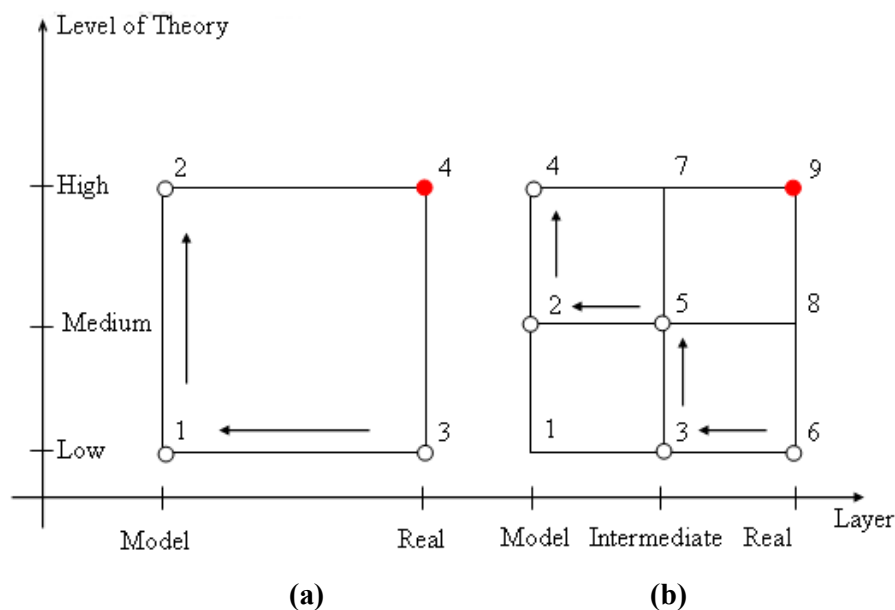


**Figure 2.4:** The ONIOM extrapolation scheme for (a) the two layered ONIOM method and (b) the three layered ONIOM method (Morokuma, 2003).

The total energy of the system is also known as ‘extrapolated energy’. For the two layered ONIOM calculation is obtained from three independent calculations as expressed in Equation 2.2 (Morokuma, 2003; Vreven & Morokuma, 2006):

$$E_{\text{ONIOM2}} = E_{\text{real,low}} - E_{\text{model,low}} + E_{\text{model,high}} = E_3 - E_1 + E_2 \quad (2.2)$$

Meanwhile, the total energy of the system for three layered ONIOM calculation is expressed as in Equation 2.3 (Morokuma, 2003).

$$\begin{aligned} E_{\text{ONIOM3}} &= E_{\text{real,low}} - E_{\text{intermediate,low}} + E_{\text{intermediate,medium}} - E_{\text{model,medium}} + E_{\text{model,high}} \\ &= E_6 - E_3 + E_5 - E_2 + E_4 \end{aligned} \quad (2.3)$$

## 2.5 Quantum Chemistry Software Packages

At present, there are many quantum chemistry softwares available such as GAMESS (Schmidt et al., 1993), AMBER (Cornell et al., 1995), Q-Chem (Kong et al., 2000), Gaussian (Frisch et al., 2004) and many more. Gaussian is one of the popular computational quantum chemistry softwares and Gaussian03 version of this software was used in this study. In 1970, John Pople with his colleagues found the Gaussian software (Frenking & Schleyer, 2004). The main idea of Gaussian is to implement Gaussian type orbitals (GTO) in order to improve the calculations performance of Slater type orbitals (STO).

The STOs are assumed located at the center of a hydrogen atom and there is only one integral exist (Jensen, 2007; Levine, 2000). However, for diatomic, triatomic and molecules with more atoms, we need to deal with two or more center integrals for the molecules (Levine, 2000) and the calculation for three- and four-center integrals cannot be done (Jensen, 2007; Levine, 2000). Therefore, STOs are mostly applied in atomic and diatomic molecules by the semi-empirical methods, where all of the three- and four-center integrals are ignored (Jensen, 2007). The Gaussian type functions is performing much faster than the Slater integral evaluation (Levine, 2000) where it uses the same functions for solving the one-electron hydrogen atom with inclusion of a polynomial in the Cartesian coordinates ( $x, y, z$ ), with an exponential in  $r^2$  (Hehre, 2003). In order to obtain results with higher accuracy, the GTOs calculations are recommended because GTOs are much more accurate compared to the STOs (Jensen, 2007).

Gaussian program can perform optimization of the molecular structures, calculation of the vibrational frequencies, some thermodynamic properties (Ochterski, 2000), search for the TS, IRC and even include a solvent effect to the system (Levine, 2000). The ab initio methods of calculation in the Gaussian software program included DFT (Bauschlicher, 1995), MP (Möller & Plesset, 1934) and HF (Pople & Nesbet, 1954) methods, semi-empirical methods included AM1 (Dewar et al., 1985), PM3 (Rzepa & Yi, 1991) and MNDO (Dewar & Li, 1974) and molecular mechanics method with universal force field (UFF) (Rappié et al., 1992) and AMBER force field (Cornell et al., 1995).

## **2.6 Theoretical Study By Applying A Hybrid QM/MM Method**

In recent years, many theoretical studies of the interactions between organic compounds and zeolites were extensively reported. The theoretically calculated adsorption energies for the organic compounds on different types of zeolite show that they are comparable with the experimental data (Boekfa et al., 2008; Houthoofd et al., 2008; Pantu et al., 2007; Lomratsiri et al., 2006; Namuangruk et al., 2006; Yuan et al., 2006; Jansang & Limtrakul, 2005; Jiang, et al., 2005; Rungsirisakun et al., 2005; Bobuatong & Limtrakul, 2003; Panjan & Limtrakul, 2003; Kasuriya et al., 2003; Raksakoon & Limtrakul 2003). For instance, the experimental results reported the adsorption energies of ethylene over the sodium faujasite (Na-FAU) (Bobuatong & Limtrakul, 2003), H-ZSM5 (Panjan & Limtrakul, 2003) and hydrogen faujasite (H-FAU) (Kasuriya et al., 2003) were -8.8, - 9.6, and -9.1 kcal/mol respectively. The theoretically calculated results are comparable with the experimental with -8.65, - 9.14 and -8.65 kcal/mol for the respective complexes.

Next, the energy of adsorption for benzene was investigated over the H-FAU (Rungsirisakun et al., 2005), H-ZSM5 (Raksakoon & Limtrakul 2003) zeolites and MCM-41 material (Jansang & Limtrakul, 2005) were found to be -15.18, -13.75 and -15.2 kcal/mol, respectively, which are comparable to the experimental data with -15.3, -13.75 and -14.4 kcal/mol, respectively. There are many reports that demonstrated the reliability of the theoretical results, such as the adsorption energies of the amines (Jiang, et al., 2005) and pyridine over a zeolite catalyst (Yuan et al., 2006). These reports also suggested that the extended zeolite frameworks gave a more reliable adsorption energy compared to the small quantum cluster model of zeolites (Houthoofd et al., 2008; Lomratsiri et al., 2006; Jansang & Limtrakul, 2005; Rungsirisakun et al., 2005; Bobuatong & Limtrakul, 2003; Panjan & Limtrakul, 2003; Kasuriya et al., 2003; Raksakoon & Limtrakul 2003).

Theoretical investigations on cracking of unsaturated hydrocarbon were done by Guo et al. (2007), Blaszkowski et al. (1996) with a simple 3T quantum cluster of zeolite while Sun et al. (2010) used an extended zeolite framework. All of these studies showed similar reaction mechanisms for the direct cracking of the unsaturated hydrocarbon. Firstly, the unsaturated hydrocarbon is adsorbed on the zeolite active site and followed by the primary carbon is attacked by a proton from the zeolite acid site. In the TS, an alkoxide ion is formed and the proton from the zeolite forms a bond with a carbon atom to release methane. Despite direct mechanism pathway for hydrocarbon cracking, Sun et al. (2010) have proposed that the dimerization cracking pathway has lower activation energy compared to the direct cracking reaction and dimerization cracking is much in favor.